CHEMISTRY OF MATERIALS
Cite This: Chem. Mater. 2018, 30, 5444−5450
Article
pubs.acs.org/cm

Linear and Cross-Linked Ionic Liquid Polymers as Binders in Lithium−Sulfur Batteries

Alen Vizintin,[†] Ryan Guterman,*[,§] Johannes Schmidt,[∥] Markus Antonietti,[§] and Robert Dominko[†,‡]

[†]National Institute of Chemistry, Hajdrihova 19, 1000 Ljubljana, Slovenia
[‡]Faculty of Chemistry and Chemical Technology, University of Ljubljana, Večna pot 113, 1000 Ljubljana, Slovenia
[§]Max Planck Institute of Colloids and Interfaces, Am Mühlenberg 1, 14476 Potsdam, Germany
[∥]Technische Universität Berlin, Institut für Chemie, Hardenbergstrasse 40, 10623 Berlin, Germany

Supporting Information

ABSTRACT: A collection of different polymeric ionic liquids (PILs) were explored as cathode binders in lithium−sulfur batteries. The PIL molecular structure, polymer backbone, and polymer architecture were found to influence the cell capacity, the cyclability, and the morphology of the cathode itself. PILs with styrene backbones performed better than the vinyl-based polymer, while cross-linked PILs imparted further improved capacities, cyclability, and reduced overpotentials. Unlike polyvinylidene fluoride, PIL binders mixed with the sulfide species, resulting in more uniformly distributed sulfides in the cathode and better sulfide transport. These features helped to mitigate volume change-induced degradation that typically plagues Li−S batteries. The uptake of polysulfides by PILs also constrains the polysulfide shuttle during battery cycling, leading to better cycling stability. While traditionally binders are viewed only as a "glue" to hold the active material together, PIL binders have additional functions and play an active role during Li−S battery working operation.

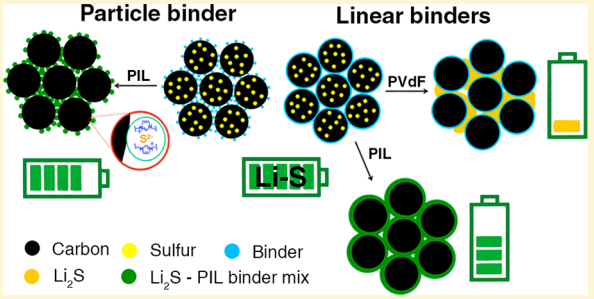

INTRODUCTION

High-performance lithium−sulfur (Li−S) batteries that are lightweight and energy dense are contenders to replace the current Li-ion technology.[1] While the potential energy storage of Li−S batteries is quite high, low cyclability arising from polysulfide migration to the anode, and/or volume changes at the cathode, significantly reduces the lifetime of such devices. For these reasons, researchers have sought to develop new electrolytes,[2−4] membranes,[5,6] cathodes,[7,8] and sulfur impregnation techniques[8] to overcome these persistent issues. In general, the role of binders in the operation of the battery has garnered less attention, despite comprising a significant portion of the total weight of the cell (5−10 wt %).[9−12] This is in light of the fact that the binder is responsible for "gluing" the components during large volume changes. Even small improvements to the overall performance of the battery can, on an industrial scale, lead to large energy savings. Polyvinylidene fluoride (PVdF) is currently the standard for lithium battery technology and is routinely used in lithium-ion and lithium−sulfur batteries for its chemical inertness and availability. Despite a number of clear issues, such as delamination from the active components, it has thus far been sufficient for the development of new battery systems. One issue that PVdF does not address is the 80% volume expansion that occurs upon formation of Li_2S. This volume change disrupts electrical contacts within the cathode, which in turn reduces cyclability.[13] An improved binder that can mitigate these issues could help to accelerate the development of Li−S batteries as a practical alternative to current technologies. A class of polymers that have recently garnered attention are polymeric ionic liquids (PILs), whose high electrochemical stability, conductivity, and good processability are well suited for electrochemical applications.[14] They have been incorporated in supercapacitors,[15] electrochemical sensors,[16,17] and a variety of energy devices[18,19] with good success. Recently, it was found that their high stability was advantageous for use as a binder in lithium-ion batteries.[20,21] Linear PILs were capable of wrapping the powder components while still allowing for Li^+ to flow, thus improving cyclability.[20] Nanoparticle PILs were found to operate according to a different mechanism by allowing the electrolyte to permeate between the free spaces.[21] During cycling, these nanoparticles would maintain contacts between the conductive components while permitting the flow of the electrolyte. In comparison, only a few studies have been conducted for the use of PILs in lithium−sulfur batteries.[22−24] While molecular interactions between ionic liquids and polysulfide species have been examined in great detail,[25−27] the role of a cationic polymer binder in similar environments is not well understood. There is strong evidence found by Helms et al. for such polymers to

Received: June 5, 2018
Revised: July 12, 2018
Published: July 13, 2018

DOI: 10.1021/acs.chemmater.8b02357
Chem. Mater. 2018, 30, 5444−5450

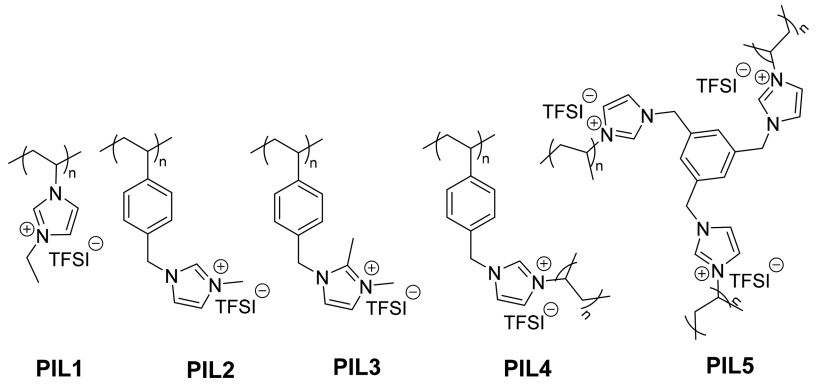

Figure 1. PIL binders examined for use in Li−S systems.

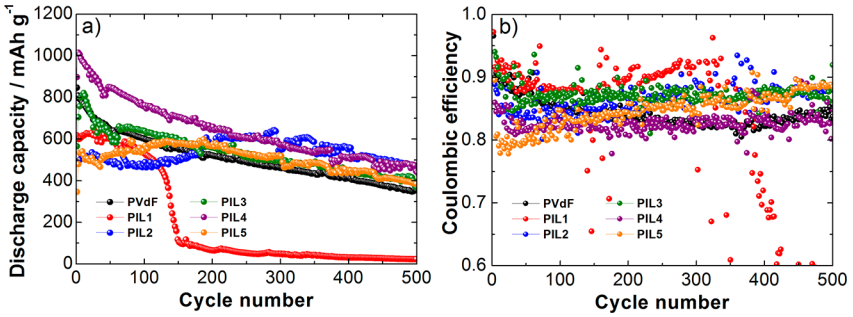

Figure 2. (a) Discharge capacity and (b) Coulombic efficiency for PVdF and **PIL1−5** in a Li−S battery at a C/5 current density.

facilitate lithium-ion transport and restrict sulfide diffusion simultaneously, which in turn leads to improved cyclability.[24] However, no study has been conducted to compare the effect of different cationic polymers or PILs. In this context, we examined five PIL binders, as linear or cross-linked nanoparticles, for their use in lithium−sulfur batteries. We found that in all cases, the PILs were generally better than PVdF with respect to cyclability, with some PILs displaying higher discharge capacities in extended cycling experiments. We found that this improvement is due to the compatibility between the PIL and the produced sulfides, which inhibits swelling-induced degradation and retention of the sulfides within the cathode. We postulate about the nature of the PIL in these batteries and demonstrate a potential route for further PIL binder exploration.

EXPERIMENTAL SECTION

Materials. Azobis(isobutyronitrile) (AIBN) was purchased from Wake Chemicals and used as received. PVdF (average M_w of 534000, CAS Registry No. 24937-79-9, Sigma-Aldrich) and Printex XE2 (Degussa) were used for electrode preparation. LiTFSI (1 M) in a TEGME/DOL mixture (purity of 99.9%, E057, Solvionic) was used as the electrolyte. Lithium foil (FMC, 500 μm) was used as the anode.

Synthesis. Linear binders **PIL1−3** and cross-linked nanoparticle binder **PIL5** were synthesized according to literature procedures.[20,21] Cross-linked nanoparticle **PIL4** was synthesized from the TFSI-based monomer[28] in methanol by precipitation polymerization. Briefly, the monomer (7.32 g, 14.90 mmol) was dissolved in methanol (50 mL) containing 1.5 wt % AIBN (0.108 g, 0.657 mmol) and stirred for 18 h at 60 °C. The precipitate was then rinsed with methanol (4 × 100 mL) to remove the excess monomer and dried *in vacuo* (Scheme S1).

Electrochemistry. Carbon (Ensaco 350G, Imerys) was ball milled for 30 min at 300 rpm with sulfur in a mass ratio of 1:2. The mixture was heated to 155 °C with a heating ramp of 0.2 °C min^{-1}, where it was kept for 5 h. Cooling to room temperature was performed at a rate of 0.5 °C min^{-1}. The electrodes were prepared by mixing the sulfur/carbon composite (66 wt % sulfur), the binder (PVdF or **PIL1−5**), and a conductive carbon black additive (Printex XE2, Degussa) in a mass ratio of 80:10:10. The slurry was prepared in *N*-methyl-2-pyrrolidine (NMP) and cast on carbon-coated aluminum foil. The typical sulfur loading on carbon-coated aluminum foil was approximately 1.5 mg of S cm^{-2}. A pouch type two-electrode cell was prepared inside an argon-filled glovebox. The sulfur cathode (2 cm^2 electrode) was separated from the metallic lithium anode with Celgard 2400 separator. The electrolyte 1 M LiTFSI in a TEGDME/DOL mixture (1:1 by volume) was normalized to 15 μL per mass of sulfur. The batteries were cycled in the potential range from 1.5 to 3.0 V by using a Biologic VMP3 galvanostat/potentiostat at a current density of C/5 (334.4 mA g^{-1}).

X-ray Photoelectron Spectroscopy (XPS). XPS measurements were performed using a Thermo Scientific K-Alpha+ X-ray photoelectron spectrometer. All samples were analyzed using a micro-focused, monochromated Al Kα X-ray source (1486.68 eV, 400 μm spot size). The K-Alpha+ charge compensation system was employed during analysis to prevent any localized charge buildup. The samples were mounted on conductive carbon tape, and the resulting spectra were analyzed using the Avantage software from Thermo Scientific.

Polysulfide Uptake. Inside an argon-filled glovebox, 100 mg of each binder (PVdF and **PIL4**) was placed into two separate vial flasks; 500 μL of 0.05 M Li_2S_2 in 1 M LiTFSI in a TEGDME/DOL solution was added to each binder-containing vial flask. The solution was left inside the glovebox for 24 h.

RESULTS AND DISCUSSION

To determine the effect of different PIL binders on the performance of Li−S batteries, three different linear polymers (**PIL1−3**) and two cross-linked polymers (**PIL4** and **PIL5**) were prepared (Figure 1). **PIL1** and **PIL2** possess vinyl and styrenic backbones, respectively, while **PIL3** is a styrenic PIL with a methyl-protected substituent at its C2 position. We also examined two cross-linked nanoparticle systems, **PIL4** and **PIL5**, that possess both different molecular structures and

DOI: 10.1021/acs.chemmater.8b02357
Chem. Mater. 2018, 30, 5444−5450

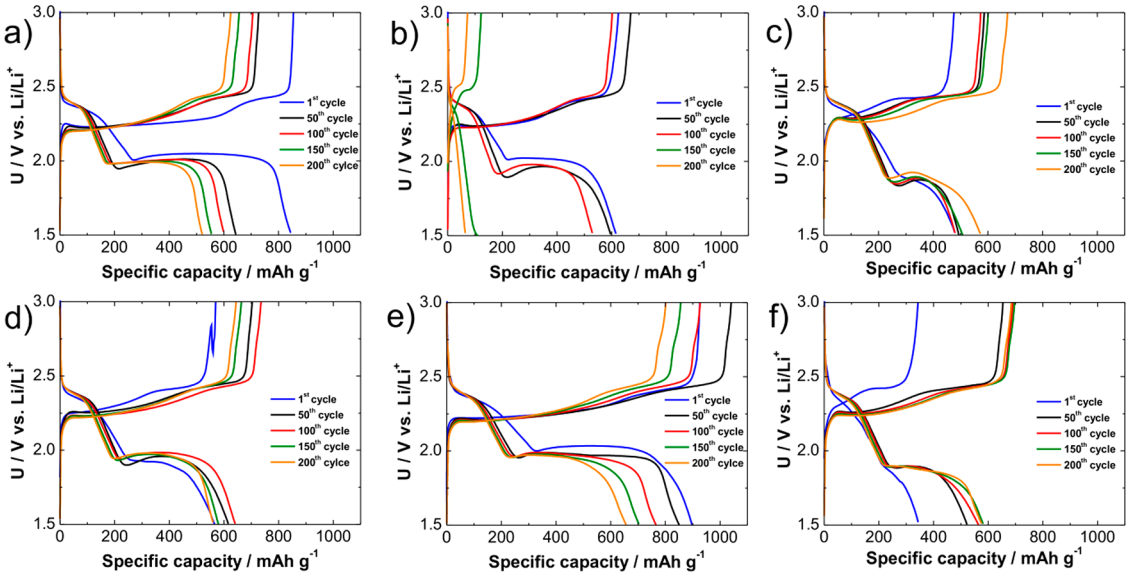

Figure 3. Galvanostatic discharge−charge voltage profiles for the Li−S cells with (a) the PVdF binder, (b) the **PIL1** binder, (c) the **PIL2** binder, (d) the **PIL3** binder, (e) the **PIL4** binder, and (f) the **PIL5** binder at a C/5 (334.4 mA g^{-1}) current density.

Table 1. Effect of the Cycling and Binders on Q_{disch}, Q_{high}/Q_{disch}, and Q_{low}/Q_{disch} Ratio and Cell Overpotential

	cycle 50				cycle 200			
binder	Q_{disch} (mAh g^{-1})	Q_{high}/Q_{disch} (%)	Q_{low}/Q_{disch} (%)	η_{tot} (mV)	Q_{disch} (mAh g^{-1})	Q_{high}/Q_{disch} (%)	Q_{low}/Q_{disch} (%)	η_{tot} (mV)
PVdF	644	34	66	146	521	35	65	152
PIL1	597	37	63	171	64	100	–	–
PIL2	494	55	45	274	574	42	58	212
PIL3	616	40	60	184	562	36	64	163
PIL4	851	31	69	122	657	38	64	140
PIL5	523	47	53	242	578	39	61	219

different numbers of polymerizable groups. These differences manifest in their size and morphology upon dispersion polymerization, with **PIL5** having an average diameter of 10−30 nm[21] and **PIL4** having a diameter of ∼20 nm and being comprised of smaller particles (∼5 nm in diameter) (Figure S1).

The electrochemical performance of **PIL1−5** and PVdF as binders was tested in a Li−S battery at a C/5 (334.4 mA g^{-1}) current density (Figure 2). PVdF is a well-known inert binder and possesses no electronic or ionic conductivity.[29] The cell with PVdF achieved an initial discharge of 847 mAh g^{-1}, which faded to 521 and 355 mAh g^{-1} after 200 and 500 cycles, respectively, with a Coulombic efficiency of approximately 83%. Figure 2 shows that PIL binders influence discharge capacities and the rate of capacity fading of the cell. **PIL1** exhibits a discharge capacity that is lower than that of PVdF; however, after prolonged discharge−charge cycling, severe capacity degradation was observed. This is not surprising as similar instabilities for **PIL1** were observed in a Li-ion battery[20] and are a result of side reactions on the ethyl substituent. Cells with **PIL2** had lower initial capacities of 482 and 494 mAh g^{-1} in the first and 50th cycle, respectively. However, after 200 cycles, an increase of 16% of the initial capacity was observed (574 mAh g^{-1}), while after 500 cycles, a discharge capacity of 473 mAh g^{-1} was observed. The cells with binders **PIL3−5** showed an increase in capacities in the initial cycles, with cells containing binder **PIL3** reaching the highest discharge capacity after 11 cycles followed by cycling behavior similar to that of PVdF. The similar performances of **PIL2** and **PIL3** indicate that methyl protection at the C2 position is not particularly important, unlike in Li-ion batteries, which benefit from C2 protection.[20] This is likely due to the lower operating voltages in Li−S versus Li-ion batteries and indicates that greater tolerance for PIL structures is possible, allowing for a greater number of PILs to be examined for these applications. The Li−S cell with **PIL4** attained the highest discharge capacity of 1015 mAh g^{-1} after three cycles, and this value was the highest among those of the binders tested. The discharge capacity of the cell with **PIL4** slowly faded to 657 and 446 mAh g^{-1} after 200 and 500 cycles, respectively. The cell with **PIL5** had the lowest initial discharge capacity; however, an increase of 10% was observed after 200 cycles with stable cycling.

Figure 3 represents the discharge and charge voltage profiles of the Li−S batteries with PVdF and **PIL1−5**. In all tested samples, two Li−S characteristic plateaus were observed; the high and the low-voltage plateau.

To facilitate the interpretation of the involved complex reactions, the voltage profile was divided into three sections, full discharge (denoted as Q_{disch}), high-voltage plateau (Q_{high}), and low-voltage plateau (Q_{low}). The high-voltage plateau (denoted as Q_{high}), from 2.5 to 1.9 V, correlates to the reduction of sulfur into long-chain and mid-chain polysulfides. The low-voltage plateau (denoted as Q_{low}), from 1.9 to 1.5 V, correlates to the equilibrium between polysulfides and precipitated Li_2S.[29−31] Similar to what Peled et al. have reported,[29] the binder influences Q_{high}, Q_{low}, and the cell overpotential (Table 1). In the case of PVdF, the Q_{high}/Q_{disch}

DOI: 10.1021/acs.chemmater.8b02357
Chem. Mater. 2018, 30, 5444−5450

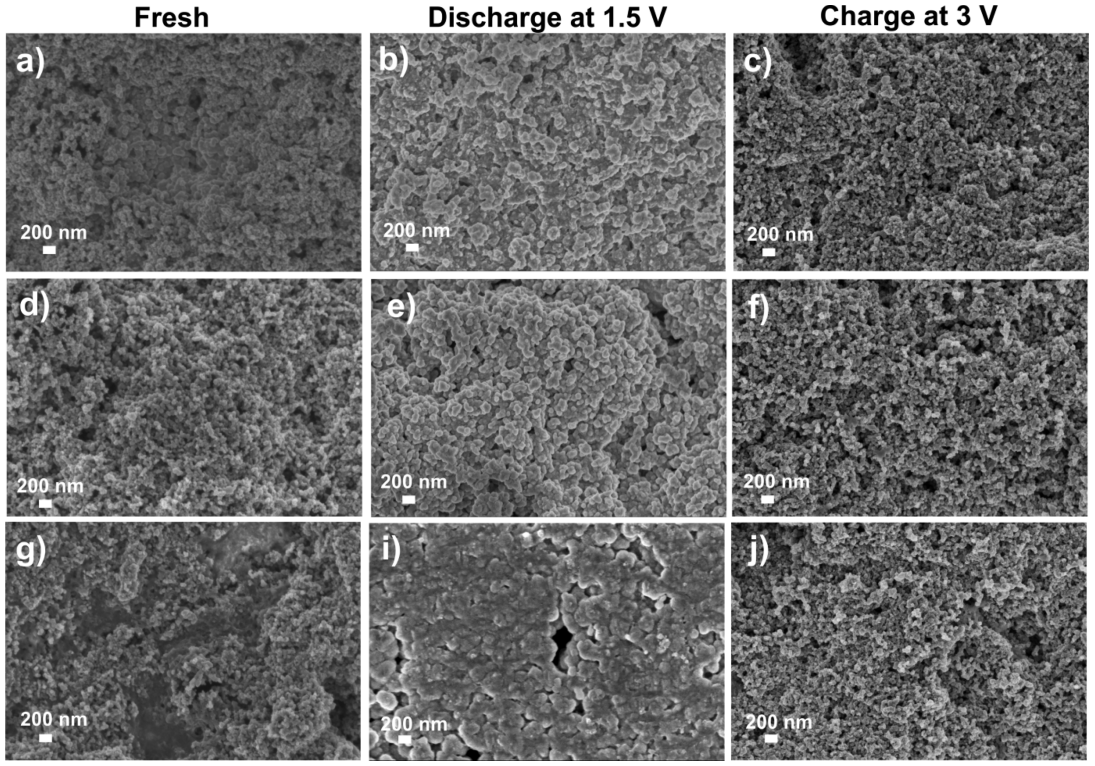

Figure 4. SEM micrographs with a higher-magnification top view for fresh sulfur cathodes and sulfur cathodes discharged at 1.5 V and charged at 3.0 V with (a–c) the PVdF binder, (d–f) **PIL2**, and (g, i, and j) **PIL4**.

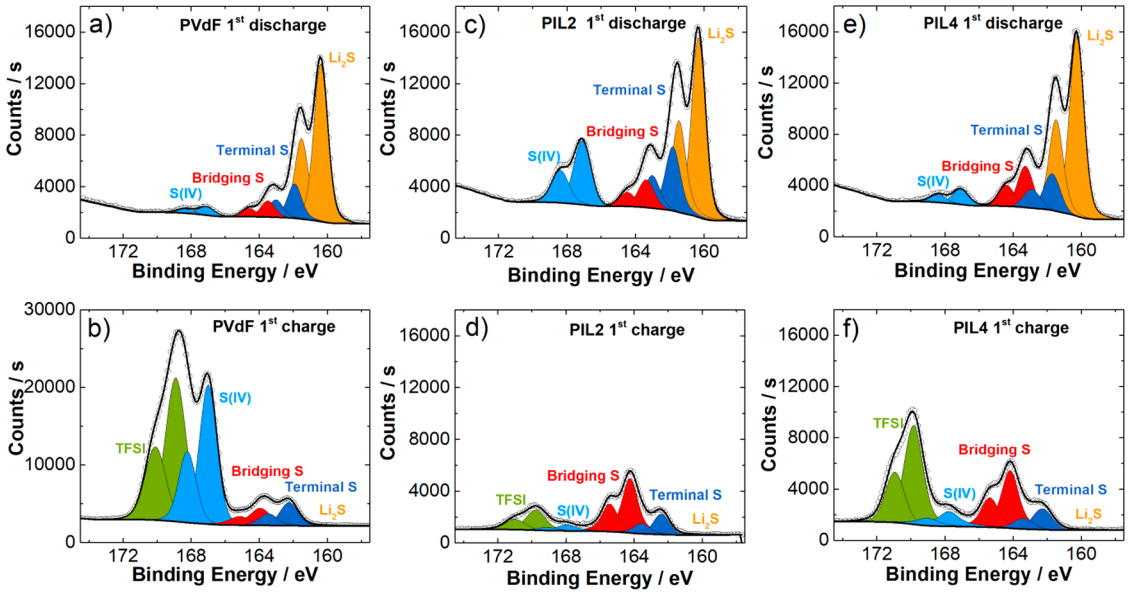

Figure 5. XPS S 2p spectra of the composite cathode with (a) PVdF in the first discharge, (b) PVdF in the first charge, (c) **PIL2** in the first discharge, (d) **PIL2** in the first charge, (e) **PIL4** in the first discharge, and (f) **PIL4** in the first charge.

ratio is approximately 30% and does not change from the 50th to 200th cycle. The constant Q_{high}/Q_{disch} ratio shows that capacity degradation is the same for the high-voltage and low-voltage plateaus, which correlates with loss of sulfur. For **PIL4**, the Q_{high}/Q_{disch} ratio increases from the 50th to 200th cycle. This may indicate that reduction of sulfur to Li_2S_4 is more efficient with prolonged discharge–charge cycling. Interestingly, with **PIL2** and **PIL5**, the Q_{high}/Q_{disch} ratio is higher in comparison to those of the other binders and is around half of Q_{disch}. However, from the 50th to 200th cycle, the Q_{high}/Q_{disch} ratio decreases to 40%. Similar behavior is observed in the obtained discharge capacities for **PIL2** and **PIL5** (Figure 2), where the capacity increases during prolonged cycling. The small initial Q_{low}/Q_{disch} ratio and its gradual increase with cycling are due to the less effective initial reduction from Li_2S_4 to Li_2S, which is an indication of an initial kinetics limitation. Furthermore, **PIL2** and **PIL5** have the highest overpotential. The similar capacity fading after 200 cycles between the PVdF and PILs binders indicates that similar degradation mecha-

DOI: 10.1021/acs.chemmater.8b02357
Chem. Mater. 2018, 30, 5444–5450

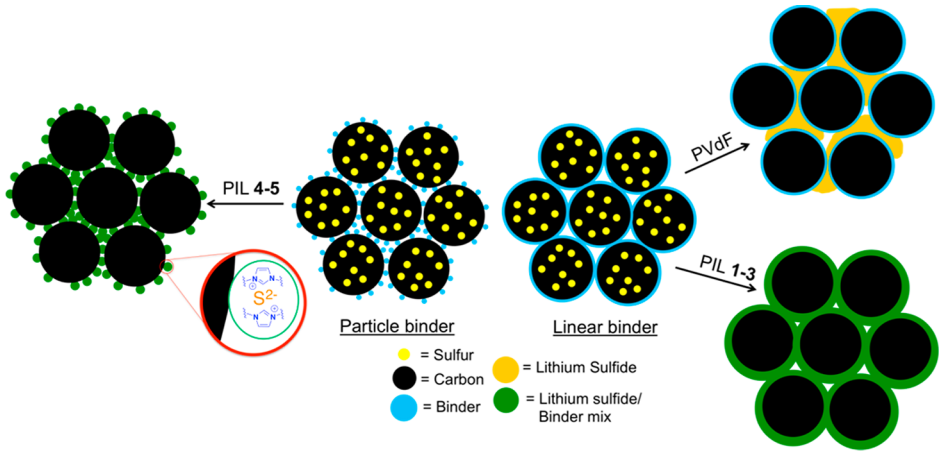

Figure 6. Schematic representation of sulfide precipitation around and between the binder/carbon for PVdF and PIL binders.

nisms occur. However, the fading with PILs is slower because of its favorable interaction with the polysulfide species.

To study the effect of the binders on the cathode morphology, post mortem scanning electron microscopy (SEM) analysis was performed on disassembled cathodes (Figure S2). SEM images of freshly discharged (1.5 V) and charged (3 V) cathodes containing PVdF, **PIL2**, and **PIL4** are shown in Figure 4. In the case of the fresh cathode with the PVdF binder, a porous cathode structure was observed with interconnected sulfur-impregnated carbon particles. The discharged cathode with PVdF shows that the pores are blocked because of the crystallization of Li_2S on the cathode surface. When charged, the open porosity is re-established due to Li_2S consumption and the re-formation of sulfur. The fresh electrode with binder **PIL2** is similar to the cathode with the PVdF binder, while the fresh cathode containing binder **PIL4** possessed a polymeric film of interconnected sulfur-impregnated carbon particles on the surface. SEM images of the discharged cathodes with **PIL2** and **PIL4** were similar to each other with a "swelled particle" structure containing open pores. This is in stark contrast to the discharged cathode containing the PVdF binder, which appears to have filled pores and no "swelling". This indicates that the growth of Li_2S is likely different in the presence of PIL and PVdF and that the improved cycling is derived from this interaction. According to Welton et al.,[32] dissolution of ionic solutes in ILs takes place via metathesis reactions, thus resulting in an intimate mixing of the two ionic components. The observed differences from SEM between the discharged PVdF and PIL samples can be explained by the uniform mixing and retention of sulfide species with the PIL binder (in the form of ion-exchange reactions), which then influences Li_2S growth and battery cycling. The fluorophilic character of PVdF does not allow any of these processes to occur and thus leads to poorer cycling stability.

Analysis of the cathodes by X-ray photoelectron spectroscopy (XPS) S 2p spectra (Figure 5) revealed that the differences in morphology observed in the SEM images are not met by differences in their surface chemical composition.

In all cases, four different components were observed in the discharged samples. They include Li_2S (around 160.5 eV) and terminal (around 162 eV) and bridging (around 163.6 eV) sulfur, and the decomposition products S(IV) from TFSI salts.[6] In addition, the TFSI anion was observed in only the charged cathodes. Thus, the stark differences between PVdF and PIL in the charged cathodes are a result of how the respective binders affect the growth of the produced sulfides. The perfluorinated structure of PVdF prefers not to mix with the sulfide salts, resulting in sulfide precipitation on top and between the binder/carbon interstitial spaces (Figure 6). This is supported by the dramatically low solubility of lithium sulfides in fluorinated solvents, which applies to the interaction between PVdF and the lithium sulfides.[24,33,34] PILs, however, have shown the ability to take up a variety of anions, direct the growth of crystalline compounds like bismuth sulfide, and generally promote the stabilization of interfaces for nanoparticle dispersions.[35−38] The more favorable interactions between the produced lithium sulfides and PIL result in a mixing of these two components, a more even distribution and volume expansion within the cathode, and thus more stable cyclability (Figure 6, bottom right). This is supported by the XPS S 2p spectra (Figure 5) of the cathodes in the charge state. On the surface of the cathode with the PVdF binder, mostly LiTFSI salts and a mixture of short-chain and mid-chain polysulfides are present, due to dissolution and shuttling of long-chain polysulfides. On the surface of the cathode with PIL binders, mostly long-chain polysulfides are found. These results support the interaction and uptake of polysulfides by PILs. Furthermore, we assume it is for this reason that the carbon particles appear to be more swolen in the SEM images for **PIL2** and **PIL4** in comparison to those for PVdF. It was also noticed that lithium sulfide sublimation occurred in the SEM vacuum chamber for the discharged cathode containing PVdF and not for PIL, indicating that the lithium sulfides are strongly bound within and/or around the PIL.[24] This effect does not appear to be different for **PIL2** and **PIL4** despite the former being a soluble homopolymer and the latter a nanoparticle binder. In contrast to this, high overpotentials were observed for **PIL2** and **PIL5** and not for **PIL4**. In the case for **PIL2**, high overpotentials are a result of inefficient electrolyte transport. This problem may be mitigated by particle binders that allow for optimal transport of electrolyte through the interstitial spaces (Figure 6, left).[21] For **PIL5**, the kinetics of Li_2S growth was hampered (Figure 3) and may stem from the more cross-linked and unswellable structure, preventing mixing with produced sulfides.

To test the swelling and polysulfide uptake of the polymers, TEGDME/DOL solutions containing 0.05 M Li_2S_2 and 1 M LiTFSI were mixed with PVdF and **PIL4** (Figure S3).[39] When the green solution was mixed with the PVdF dispersion, the

DOI: 10.1021/acs.chemmater.8b02357
Chem. Mater. 2018, 30, 5444−5450

color of the solution remained unchanged after 24 h (Figure S3a). When the polysulfide solution was mixed with a dispersion of **PIL4**, the PIL noticeably swelled and the color of the solution changed from green to orange (Figure S3b). The change in color from green to orange suggests a chemical reaction between **PIL4** and Li_2S_2, meaning **PIL4** acts as a catalyst for the disproportionation reaction of Li_2S_2[40,41] as presented in the following reaction:

$$3S_2^{2-} \leftrightarrow S_4^{2-} + 2S^{2-}$$

After 24 h, **PIL4** was swolen and absorbed the polysulfide solution, forming a white gel. The ability of the particles to reversibly swell and deswell allows for their use as "sulfide reservoirs" during cycling. This feature combined with their effective electrolyte transport demonstrates an improved approach for PIL utilization in lithium−sulfur battery systems.

In Li−S batteries, the role of the PIL binder is not only to "glue" the active material together but also to play an active role during cycling. They efficiently improve the reduction of sulfur into lithium polysulfides and improve the redistribution of Li_2S over the carbon surface. Furthermore, PIL-based binders can reduce volume change-induced stress by taking up and/or releasing lithium polysulfides during swelling and deswelling cycles.

CONCLUSIONS

In conclusion, five different PILs were used as binders in lithium−sulfur batteries and compared to conventional PVdF. The PIL binders possessed different chemical structures, polymer backbones, and polymeric architectures, including linear homopolymers and nanoparticles. We found that in all cases, PILs were equal or superior to PVdF with respect to cyclability, with some PILs displaying higher discharge capacities across the tested lifetime. The PIL binders improved the reduction of sulfur into Li_2S_4 more efficiently while simultaneously improving the redistribution of Li_2S in the cathode, which boosted battery cyclability. We can conclude that the key to this improved performance is a result of the favorable interactions between the PIL and the produced lithium sulfide species, resulting in mixing of the two and a more even volume expansion during discharge. This is in contrast to PVdF, which does not mix with the lithium sulfide species, resulting in uneven volume expansion between the carbon particles. Such added stress within the cathode results in a shorter lifetime with respect to their PIL counterparts. Finally, we show that PIL nanoparticles lower the resistance of the cell in comparison to that seen with PIL homopolymers by promoting the flow of the electrolyte between the carbon particles during cycling. This is a result of their small size, large surface area, swellability for the produced lithium sulfide species, and improved electrolyte transport through the interstitial spaces. Furthermore, the PIL nanoparticles promoted the disproportionation reaction of the weakly soluble short-chain polysulfides into long-chain polysulfides, which has a beneficial influence on the achieved capacities. These findings illustrate the positive effects of using PILs in lithium−sulfur batteries and will aid the search for optimized binder designs. Future work will also examine how Li_2S crystal growth is influenced by the presence of PIL.

ASSOCIATED CONTENT

Supporting Information

The Supporting Information is available free of charge on the ACS Publications website at DOI: 10.1021/acs.chemmater.8b02357.

A synthetic scheme, SEM images, and comparison photos of the swolen binders (PDF)

AUTHOR INFORMATION

Corresponding Author

*E-mail: ryan.guterman@mpikg.mpg.de.

ORCID

Alen Vizintin: 0000-0003-1876-1396

Ryan Guterman: 0000-0003-3231-6176

Robert Dominko: 0000-0002-6673-4459

Funding

The European Union Horizon 2020 framework under Grant Agreement 666221 (HELIS) and ARRS Program P2-0393 are acknowledged for funding.

Notes

The authors declare no competing financial interest.

ACKNOWLEDGMENTS

The authors thank all members of HELIS who contributed through their constructive discussion. The authors also thank the Max Planck Society and the National Institute of Chemistry (Slovenia) for their ongoing support.

REFERENCES

(1) Bruce, P. G.; Freunberger, S. A.; Hardwick, L. J.; Tarascon, J. M. Li−O_2 and Li−S Batteries with High Energy Storage. *Nat. Mater.* **2012**, *11*, 19−29.

(2) Scheers, J.; Fantini, S.; Johansson, P. A Review of Electrolytes for Lithium−sulphur Batteries. *J. Power Sources* **2014**, *255*, 204−218.

(3) Zhang, S.; Ueno, K.; Dokko, K.; Watanabe, M. Recent Advances in Electrolytes for Lithium-Sulfur Batteries. *Adv. Energy Mater.* **2015**, *5*, 1500117.

(4) Drvarič Talian, S.; Jeschke, S.; Vizintin, A.; Pirnat, K.; Arčon, I.; Aquilanti, G.; Johansson, P.; Dominko, R. Fluorinated Ether Based Electrolyte for High-Energy Lithium−Sulfur Batteries: Li^+ Solvation Role Behind Reduced Polysulfide Solubility. *Chem. Mater.* **2017**, *29*, 10037−10044.

(5) Vizintin, A.; Patel, M. U. M.; Genorio, B.; Dominko, R. Effective Separation of Lithium Anode and Sulfur Cathode in Lithium-Sulfur Batteries. *ChemElectroChem* **2014**, *1*, 1040−1045.

(6) Vizintin, A.; Lozinšek, M.; Chellappan, R. K.; Foix, D.; Krajnc, A.; Mali, G.; Drazic, G.; Genorio, B.; Dedryvère, R.; Dominko, R. Fluorinated Reduced Graphene Oxide as an Interlayer in Li−S Batteries. *Chem. Mater.* **2015**, *27*, 7070−7081.

(7) Yang, Y.; Zheng, G.; Cui, Y. Nanostructured Sulfur Cathodes. *Chem. Soc. Rev.* **2013**, *42*, 3018−3032.

(8) Manthiram, A.; Fu, Y.; Chung, S.-H.; Zu, C.; Su, Y.-S. Rechargeable Lithium−Sulfur Batteries. *Chem. Rev.* **2014**, *114*, 11751−11787.

(9) Kovalenko, I.; Zdyrko, B.; Magasinski, A.; Hertzberg, B.; Milicev, Z.; Burtovyy, R.; Luzinov, I.; Yushin, G. A Major Constituent of Brown Algae for Use in High-Capacity Li-Ion Batteries. *Science* **2011**, *334*, 75−79.

(10) Komaba, S.; Matsuura, Y.; Ishikawa, T.; Yabuuchi, N.; Murata, W.; Kuze, S. Redox Reaction of Sn-Polyacrylate Electrodes in Aprotic Na Cell. *Electrochem. Commun.* **2012**, *21*, 65−68.

(11) Amanchukwu, C. V.; Harding, J. R.; Shao-Horn, Y.; Hammond, P. T. Understanding the Chemical Stability of Polymers for Lithium−Air Batteries. *Chem. Mater.* **2015**, *27*, 550−561.

DOI: 10.1021/acs.chemmater.8b02357
Chem. Mater. 2018, 30, 5444−5450

(12) Park, S.-J.; Zhao, H.; Ai, G.; Wang, C.; Song, X.; Yuca, N.; Battaglia, V. S.; Yang, W.; Liu, G. Side-Chain Conducting and Phase-Separated Polymeric Binders for High-Performance Silicon Anodes in Lithium-Ion Batteries. *J. Am. Chem. Soc.* **2015**, *137*, 2565−2571.
(13) Waluś, S.; Offer, G.; Hunt, I.; Patel, Y.; Stockley, T.; Williams, J.; Purkayastha, R. Volumetric Expansion of Lithium-Sulfur Cell during Operation − Fundamental Insight into Applicable Characteristics. *Energy Storage Mater.* **2018**, *10*, 233−245.
(14) Appetecchi, G. B.; Kim, G. T.; Montanino, M.; Carewska, M.; Marcilla, R.; Mecerreyes, D.; De Meatza, I. Ternary Polymer Electrolytes Containing Pyrrolidinium-Based Polymeric Ionic Liquids for Lithium Batteries. *J. Power Sources* **2010**, *195*, 3668−3675.
(15) Kim, T. Y.; Lee, H. W.; Stoller, M.; Dreyer, D. R.; Bielawski, C. W.; Ruoff, R. S.; Suh, K. S. High-Performance Supercapacitors Based on Poly(ionic Liquid)-Modified Graphene Electrodes. *ACS Nano* **2011**, *5*, 436−442.
(16) Tung, T. T.; Castro, M.; Kim, T. Y.; Suh, K. S.; Feller, J. F. High Stability Silver Nanoparticles-Graphene/poly(ionic Liquid)-Based Chemoresistive Sensors for Volatile Organic Compounds' Detection. *Anal. Bioanal. Chem.* **2014**, *406*, 3995−4004.
(17) Li, Y.; Li, G.; Wang, X.; Zhu, Z.; Ma, H.; Zhang, T.; Jin, J. Poly(ionic Liquid)-Wrapped Single-Walled Carbon Nanotubes for Sub-Ppb Detection of CO_2. *Chem. Commun.* **2012**, *48*, 8222−8224.
(18) Qiu, B.; Lin, B.; Yan, F. Ionic Liquid/poly(ionic Liquid)-Based Electrolytes for Energy Devices. *Polym. Int.* **2013**, *62*, 335−337.
(19) Lin, B.; Feng, T.; Chu, F.; Zhang, S.; Yuan, N.; Qiao, G.; Ding, J. Poly(ionic Liquid)/ionic Liquid/graphene Oxide Composite Quasi Solid-State Electrolytes for Dye Sensitized Solar Cells. *RSC Adv.* **2015**, *5*, 57216−57222.
(20) Lee, J. S.; Sakaushi, K.; Antonietti, M.; Yuan, J. Poly(ionic Liquid) Binders as Li^+ Conducting Mediators for Enhanced Electrochemical Performance. *RSC Adv.* **2015**, *5*, 85517−85522.
(21) Yuan, J.; Prescher, S.; Sakaushi, K.; Antonietti, M. Novel Polyvinylimidazolium Nanoparticles as High-Performance Binders for Lithium-Ion Batteries. *J. Mater. Chem. A* **2015**, *3*, 7229−7234.
(22) Baloch, M.; Vizintin, A.; Chellappan, R. K.; Moskon, J.; Shanmukaraj, D.; Dedryvère, R.; Rojo, T.; Dominko, R. Application of Gel Polymer Electrolytes Based on Ionic Liquids in Lithium-Sulfur Batteries. *J. Electrochem. Soc.* **2016**, *163*, A2390−A2398.
(23) Su, H.; Fu, C.; Zhao, Y.; Long, D.; Ling, L.; Wong, B. M.; Lu, J.; Guo, J. Polycation Binders: An Effective Approach toward Lithium Polysulfide Sequestration in Li−S Batteries. *ACS Energy Lett.* **2017**, *2*, 2591−2597.
(24) Li, L.; Pascal, T. A.; Connell, J. G.; Fan, F. Y.; Meckler, S. M.; Ma, L.; Chiang, Y.-M.; Prendergast, D.; Helms, B. A. Molecular Understanding of Polyelectrolyte Binders That Actively Regulate Ion Transport in Sulfur Cathodes. *Nat. Commun.* **2017**, *8*, 2277.
(25) Park, J. W.; Ueno, K.; Tachikawa, N.; Dokko, K.; Watanabe, M. Ionic Liquid Electrolytes for Lithium−Sulfur Batteries. *J. Phys. Chem. C* **2013**, *117*, 20531−20541.
(26) Dokko, K.; Tachikawa, N.; Yamauchi, K.; Tsuchiya, M.; Yamazaki, a.; Takashima, E.; Park, J.-W.; Ueno, K.; Seki, S.; Serizawa, N.; et al. Solvate Ionic Liquid Electrolyte for Li-S Batteries. *J. Electrochem. Soc.* **2013**, *160*, A1304−A1310.
(27) Salitra, G.; Markevich, E.; Rosenman, A.; Talyosef, Y.; Aurbach, D.; Garsuch, A. High-Performance Lithium-Sulfur Batteries Based on Ionic-Liquid Electrolytes with Bis(fluorolsufonyl)imide Anions and Sulfur-Encapsulated Highly Disordered Activated Carbon. *ChemElectroChem* **2014**, *1*, 1492−1496.
(28) Wilke, A.; Yuan, J.; Antonietti, M.; Weber, J. Enhanced Carbon Dioxide Adsorption by a Mesoporous Poly(ionic Liquid). *ACS Macro Lett.* **2012**, *1*, 1028−1031.
(29) Peled, E.; Goor, M.; Schektman, I.; Mukra, T.; Shoval, Y.; Golodnitsky, D. The Effect of Binders on the Performance and Degradation of the Lithium/Sulfur Battery Assembled in the Discharged State. *J. Electrochem. Soc.* **2017**, *164*, A5001−A5007.
(30) Dominko, R.; Patel, M. U. M.; Lapornik, V.; Vizintin, A.; Koželj, M.; N. Tušar, N.; Arčon, I.; Stievano, L.; Aquilanti, G. Analytical Detection of Polysulfides in the Presence of Adsorption Additives by Operando X-Ray Absorption Spectroscopy. *J. Phys. Chem. C* **2015**, *119*, 19001−19010.
(31) Kavčič, M.; Bučar, K.; Petric, M.; Žitnik, M.; Arčon, I.; Dominko, R.; Vizintin, A. Operando Resonant Inelastic X-Ray Scattering: An Appropriate Tool to Characterize Sulfur in Li−S Batteries. *J. Phys. Chem. C* **2016**, *120*, 24568−24576.
(32) Lui, M. Y.; Crowhurst, L.; Hallett, J. P.; Hunt, P. A.; Niedermeyer, H.; Welton, T. Salts Dissolved in Salts: Ionic Liquid Mixtures. *Chem. Sci.* **2011**, *2*, 1491−1469.
(33) Vizintin, A.; Chabanne, L.; Tchernychova, E.; Arčon, I.; Stievano, L.; Aquilanti, G.; Antonietti, M.; Fellinger, T. P.; Dominko, R. The Mechanism of Li_2S Activation in Lithium-Sulfur Batteries: Can We Avoid the Polysulfide Formation. *J. Power Sources* **2017**, *344*, 208−217.
(34) He, M.; Yuan, L.X. X.; Zhang, W.-X. X.; Hu, X.L. L.; Huang, Y.H. H. Enhanced Cyclability for Sulfur Cathode Achieved by a Water-Soluble Binder. *J. Phys. Chem. C* **2011**, *115*, 15703−15709.
(35) Hu, X.; Huang, J.; Zhang, W.; Li, M.; Tao, C.; Li, G. Photonic Ionic Liquids Polymer for Naked-Eye Detection of Anions. *Adv. Mater.* **2008**, *20*, 4074−4078.
(36) Gao, M. R.; Yu, S. H.; Yuan, J.; Zhang, W.; Antonietti, M. Poly(ionic Liquid)-Mediated Morphogenesis of Bismuth Sulfide with a Tunable Band Gap and Enhanced Electrocatalytic Properties. *Angew. Chem., Int. Ed.* **2016**, *55*, 12812−12816.
(37) Wu, B.; Hu, D.; Kuang, Y.; Liu, B.; Zhang, X.; Chen, J. Functionalization of Carbon Nanotubes by an Ionic-Liquid Polymer: Dispersion of Pt and PtRu Nanoparticles on Carbon Nanotubes and Their Electrocatalytic Oxidation of Methanol. *Angew. Chem., Int. Ed.* **2009**, *48*, 4751−4754.
(38) Sun, J. K.; Kochovski, Z.; Zhang, W.-Y.; Kirmse, H.; Lu, Y.; Antonietti, M.; Yuan, J. General Synthetic Route toward Highly Dispersed Metal Clusters Enabled by Poly(ionic Liquid)s. *J. Am. Chem. Soc.* **2017**, *139*, 8971−8976.
(39) Patel, M. U. M.; Dominko, R. Application of In Operando UV/Vis Spectroscopy in Lithium-Sulfur Batteries. *ChemSusChem* **2014**, *7*, 2167−2175.
(40) Wild, M.; O'Neill, L.; Zhang, T.; Purkayastha, R.; Minton, G.; Marinescu, M.; Offer, G. J. Lithium Sulfur Batteries, a Mechanistic Review. *Energy Environ. Sci.* **2015**, *8*, 3477−3494.
(41) Moy, D.; Manivannan, A.; Narayanan, S. R. Direct Measurement of Polysulfide Shuttle Current: A Window into Understanding the Performance of Lithium-Sulfur Cells. *J. Electrochem. Soc.* **2015**, *162*, A1−A7.

DOI: 10.1021/acs.chemmater.8b02357
Chem. Mater. 2018, 30, 5444−5450